Fluoromethylene Cyanate Ester Resins. Synthesis, Characterization, and Fluoromethylene Chain Length Effects

Arthur W. Snow* and Leonard J. Buckley

Naval Research Laboratory, Washington, D.C. 20375

Received August 6, 1996; Revised Manuscript Received November 21, 1996[⊗]

ABSTRACT: Fluoromethylene cyanate ester resins derived from the monomer series N≡CO−$CH_2(CF_2)_n$-CH_2−OC≡N (where n = 3, 4, 6, 8, and 10) have been synthesized and characterized. Monomer melting points range from −8 to 181 °C, and characterization includes ^{1}H, ^{13}C, and ^{19}F NMR and IR spectroscopy and DSC. Purification is a critical requirement for melt processing. The thermal curing reaction is a cyclotrimerization reaction of the cyanate functional group to the cyanurate heterocycle. Physical properties of resin castings and their variation with an increase in fluoromethylene sequence length from 3 to 10 CF_2 units include density, 1.77−1.91 g/cm^3; critical surface tension, 40−23 dyn/cm; refractive index, 1.447−1.382; dielectric constant, 2.7−2.3; 100 °C immersion water absorption, 1.67−0.68%; T_g, 84−101 °C; glass/rubber thermal expansion coefficient, (109/238−152/275 ppm/ °C; and gravimetric thermal stability, 0.0196−0.0064% weight loss/min at 300 °C). Compared with aromatic cyanate ester resins, the fluoromethylene cyanate esters have significantly lower T_g, dielectric constant, critical surface tension, and water absorption. For low-dielectric applications, the optimum trade-off between properties and processing occurs at a fluoromethylene chain length of 6.

Introduction

As a class of thermoset resins, cyanate esters are almost exclusively limited to those based on aromatic cyanate ester monomers. The fluoromethylene cyanate ester thermoset system depicted in Figure 1 is relatively novel in that the aromatic structural unit of most cyanate monomers is absent and that a variable and a potentially very large amount of fluorine may be incorporated. The loss of aromatic character and the incorporation of fluorine affects many aspects of a thermoset system, ranging from monomer syntheses and curing through a series of thermoset properties (thermal, moisture absorption, optical, wetting, adhesive, dielectric, and mechanical properties). The intent of this work is to survey this property variation as the number of fluoromethylene groups increases from 3 to 10. This fluoromethylene cyanate ester system is abbreviated FnCy, where n is the number of CF_2 units in the fluoromethylene sequence. It is further intended to index the properties of this FnCy system against a reference fluorinated aromatic cyanate resin. The reference resin chosen is based on the dicyanate of 6F-bisphenol A, which is commercially known as AroCy F (shown below).

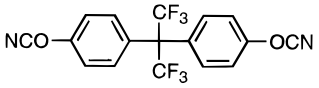

Historically, when the discovery of a general synthesis of stable aryl cyanate esters was disclosed, Grigat and Pütter additionally disclosed that cyanate esters of strongly acidic alcohols such as trihaloethanols were analogously synthesizable and similar in stability and chemistry to aryl cyanates.[1,2] In contrast, polymerizable hydrocarbon aliphatic cyanate esters have not been successfully synthesized. Simple alkyl cyanates, while synthesizable under mild conditions by other routes,[3] are unstable at ambient temperatures and rearrange to isocyanates and react to form other complex products.[4] The stability of the cyanate functional group is derived from a resonance or an electron withdrawal stabilization effect from a respective aromatic or haloalkyl structure to which it is bonded. Beyond patenting monofunctional trihaloethyl cyanates, Bayer AG did not pursue the prospects of thermosets from polyfunctional haloalkyl cyanates. In 1972, 3M Co. obtained patents on the synthesis of fluorinated aliphatic dicyanates and their thermal cure to plastic or elastomeric materials.[5] However, the monomers reported were not isolated in pure form or rigorously characterized, nor were quantitative properties reported for the thermally cured resins. Also, the fluoromethylene sequences were limited to 3 and 4 units. The current availability of fluorinated diol precursors with n = 6, 8, and 10 offers new prospects for enhanced fluorocarbon properties.

Our interest in the fluoromethylene dicyanate resin system is focused on its merit as a very low dielectric, easily processible thermoset resin system for microelectronic and electromagnetic transmission applications. Currently, these applications are the major market niche for the commercialized aromatic cyanate ester resins.[6] The low-dielectric character of these resins has been attributed to the high degree of symmetry in the cyanurate linkage structure, where dipoles associated with the carbon−nitrogen and carbon−oxygen bonds are counterbalanced resulting in a low dipole moment and a low energy storage in an electric field.[7] The fluoromethylene cyanate ester system of this study incorporates this low dipole structural feature and replaces the aromatic connecting groups by fluoromethylene connecting sequences, with the intent of further depressing the dielectric constant. Another factor is the influence of free volume, which, with a dielectric constant of 1, can be an effective diluent of a dielectric medium. As represented by the two-dimensional extended chain sketch in the lower part of Figure 1, a combination of the steric restriction of the triazine network junction and stiffness of connecting fluoromethylene chains might result in a low molecular packing density and provide an additional mechanism for lowering the dielectric constant. Ideally, at some moderate fluoromethylene chain length, this resin would have the dielectric properties of Teflon coupled with the mechanical, thermal, and processing characteristics of a good

[⊗] Abstract published in *Advance ACS Abstracts,* January 15, 1997.

S0024-9297(96)01182-5

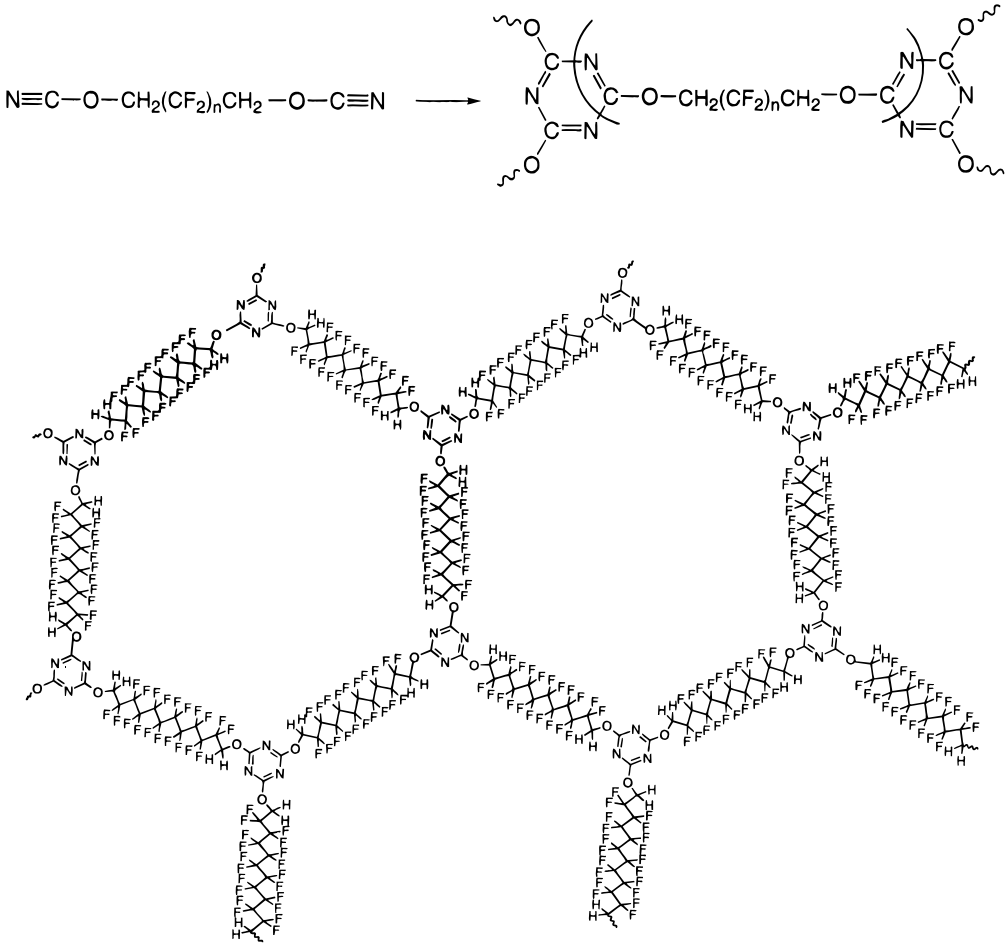

Figure 1. Fluoromethylene cyanate ester structures and curing reaction. The structure in the lower part of the figure is a two-dimensional representation of the F*n*Cy ($n = 10$) network, conceptually illustrating how a cyanurate junction connected by a stiff fluoromethylene chain might sterically generate free volume effects.

epoxy. With respect to low-dielectric applications, this fluoromethylene-linked cyanurate thermoset structure appears to possess the features of high symmetry, low polar content, and low polarizibility prescribed as desirable for low-dielectric thermoset resins.[8] Further, it represents a simple single-component system that can be processed from a stable prepolymer form of variable molecular weight. The objective of the present work is to develop a detailed synthesis and characterization for the fluoromethylene dicyanate series of monomers and corresponding thermosets, to measure and compare the physical properties of this F*n*Cy resin series with those of AroCy F and to determine at what fluoromethylene chain length an optimum trade-off between properties and processing is reached.

Experimental Section

General Information. All reagents and solvents were of reagent-grade quality, purchased commercially, and used without further purification unless otherwise noted.

Infrared spectra of monomers were obtained from samples deposited as oils or evaporated thin films on NaCl plates and from polymers as thin films cured between NaCl plates or as fine particulates dispersed in KBr. IR spectra were recorded using a Nicolet Magna FTIR 750.

^{1}H, ^{13}C, and ^{19}F NMR spectra of monomers, precursors, and prepolymers were recorded using a Bruker AC300. Acetone-d_6 was used as solvent, and the chemical shifts are internally referenced to tetramethylsilane (0 ppm), CD_3COCD_3 (29.8 ppm), and $CFCl_3$ (0 ppm) for the respective ^{1}H, ^{13}C, and ^{19}F nuclei.

Density measurements were made on void-free 0.5−0.6 g castings according to the ASTM D 792-66 displacement method at 23 °C.

Refractive index measurements on the cured resin castings were made using a Bausch & Lomb Abbe-3L refractometer at the sodium D line ($\lambda = 589$ nm). The instrument was calibrated with a standard glass test piece provided by the manufacturer. Resin castings were sanded on one side to an optically flat surface and polished with Carbimet abrasive and polishing disks to reduce scattering to a level acceptable for the contrast necessary for the measurement. Methylene iodide was used as the contact oil between the polished casting and refractometer prism. The measurement temperature was 25 °C.

Differential scanning calorimetry (DSC) data were recorded on a DuPont 2100 thermal analysis system/910 DSC module from 20−30 mg samples (prepared by curing in the DSC pan) under a nitrogen atmosphere at 10 °C/min scan rate. Monomer and diol precursor melting points were determined at the onset of the melting endotherm.

Thermogravimetric analysis (TGA) data were recorded on a DuPont 2100 thermal analysis system/951 TGA module from 10−15 mg solid samples in a nitrogen atmosphere under 300 °C isothermal and under 10 °C/min scanning conditions.

Thermomechanical analysis (TMA) data were recorded on a Perkin Elmer Series 7 thermal analysis system/TMA 7 thermomechanical analyzer in a helium atmosphere on samples under a static probe force of 20 dyn and at a heating rate of 2 °C/min. The instrument was calibrated with an aluminum expansion standard. Samples were 7.6 mm diameter disks of uniform thickness (ranging from 2 to 3 mm) which were cut by a diamond saw from cylindrical castings.

Electric field permittivity measurements (1 MHz−1.8 GHz frequency range) were made at 23 °C by an electrode contact

method using an HP4291A impedance/material analyzer. Samples were 12 mm diameter disks of uniform thickness (ranging from 1.4 to 1.8 mm) which were cut by a diamond saw from cylindrical castings. The disk is inserted into a spring-loaded parallel electrode arrangement, where a complex admittance is measured and used to calculate the complex permittivity according to[9]

$$\epsilon^* = Yt/f\epsilon_0 A \quad (1)$$

where ϵ^* is the complex permittivity, Y is the complex admittance, t is the sample thickness, f is the frequency, ϵ_0 is the permittivity of free space, and A is the electrode contact area. The apparatus is calibrated over the entire frequency range using an open and short circuit, 50 Ω load, and a low loss capacitor. This was then checked by measurements on standard materials (i.e., polyethylene and polytetrafluoroethylene).

The complex permittivity, ϵ^*, is a material property that includes the real and imaginary parts as shown in eq 2:[10]

$$\epsilon^* = \epsilon' - j\epsilon'' \quad (2)$$

where ϵ' is the real permittivity or dielectric constant and ϵ'' is the imaginary permittivity or dielectric loss. Physically, ϵ' can be understood as the energy stored per cycle, while ϵ'' is the energy dissipated per cycle.

The conditions for the water absorption experiment were immersion of 1.5 mm thick castings in 100 °C distilled water for a 96 h duration. Successive mass measurements of absorbed water were made by periodically removing castings from the water bath, blotting dry, weighing, and returning to the water bath within 5 min. Castings treated as above for the "wet dielectric constant" measurements were stored immersed in 23 °C water prior to the measurement (less than 2 days).

Contact angle measurements were made using an ASC Products 2500 video contact angle system at 23 °C. Droplets of liquids (0.5 μL) were deposited on flat clean casting surfaces, and contact angles were measured after a 15−20 s spreading time. Purified liquids with varying surface tension utilized in this measurement included: water, triple distilled, 72.8 dyn/cm; formamide, alumina column eluted, 58.2 dyn/cm; methylene iodide, alumina column eluted, 50.8 dyn/cm; *o*-tricresyl phosphate, alumina column eluted, 40.9 dyn/cm; and dicyclohexyl, alumina column eluted, 32.8 dyn/cm.

The commercial cyanate resin monomers AroCy B (2,2-bis(4-cyanatophenyl)propane) and AroCy F (2,2-bis(4-cyanatophenyl)-1,1,1,3,3,3-hexafluoropropane) were generously contributed by David A. Shimp of Ciba Geigy.

Reagents for Monomer Synthesis. Reagents and solvents for the cyanation reaction were purified as follows: fluorinated diols, see below; triethylamine, distilled (1 atm/nitrogen); cyanogen bromide *(Caution: toxic!)*, dried over anhydrous $CaCl_2$ and distilled; and acetone, dried over freshly activated 3 Å molecular sieves (12 h) and distilled (1 atm/nitrogen).

Fluorinated diols ($HOCH_2(CF_2)_nCH_2OH$, n = 3, 4, 6, 8, and 10; F3-diol, F4-diol, F6-diol, F8-diol, and F10-diol, Respectively). The n = 3 member of the series was obtained from PCR, Inc. and was purified by vacuum distillation (108 °C/10 Torr) and vacuum drying (23 °C/>12 h). The remaining members were obtained from Exfluor Research Corp. and were vacuum dried (23 °C/>12 h) before use. These compounds were analyzed by GC, DSC, and NMR. The vacuum drying effectively removed absorbed water. No evidence of incomplete fluorination in the fluoromethylene sequences or loss of alcohol difunctionality was found. Melting points and NMR analyses are as follows.

F3-diol: mp 74 °C; ^{1}H NMR (300 MHz, 16% (w/w) CD_3COCD_3) δ 4.02 (t, J_{HF} = 15 Hz), 5.00 (s, OH); ^{13}C NMR (75.5 MHz, 16% (w/w) CD_3COCD_3) δ 59.6 (t, J_{CH} = 26 Hz), 111.3 (Tquint, J_{CF} = 213 and 32 Hz), 116.2 (Tt, J_{CF} = 254 and 30 Hz); ^{19}F NMR (282 MHz, 16% (w/w) CD_3COCD_3) δ −124.63 (2F), −125.93 (1F).

F4-diol: mp 63 °C; ^{1}H NMR (300 MHz, 20% (w/w) CD_3COCD_3) δ 4.06 (t, J_{HF} = 15 Hz), 5.08 (s, OH); ^{13}C NMR (75.5 MHz, 20% (w/w) CD_3COCD_3) δ 59.8 (t, J_{CH} = 25 Hz), 112.0 (Tquint, J_{CF} = 213 and 33 Hz), 116.3 (Tt, J_{CF} = 263 and 29 Hz); ^{19}F NMR (282 MHz, 20% (w/w) CD_3COCD_3) δ −121.79 (2F), −123.55 (2F).

F6-diol: mp 43 and 84 °C (two melting points); ^{1}H NMR (300 MHz, 18% (w/w) CD_3COCD_3) δ 4.08 (t, J_{HF} = 15 Hz), 5.10 (s, OH); ^{13}C NMR (75.5 MHz, 18% (w/w) CD_3COCD_3) δ 60.1 (t, J_{CH} = 25 Hz), 111.7 (Tquint, J_{CF} = 213 and 33 Hz), 115.3, 116.7 (Tt, J_{CF} = 231 and 25 Hz); ^{19}F NMR (282 MHz, 20% (w/w) CD_3COCD_3) δ −121.54 (2F), −121.81 (2F), −123.22 (2F).

F8-diol: mp 130 °C; ^{1}H NMR (300 MHz, 17% (w/w) CD_3COCD_3) δ 4.10 (t, J_{HF} = 14 Hz), 5.30 (s, OH); ^{13}C NMR (75.5 MHz, 17% (w/w) CD_3COCD_3) δ 59.9 (t, J_{CH} = 25 Hz), 111.5 (Tquint, J_{CF} = 241 and 32 Hz), 115.4, 116.6 (Tt, J_{CF} = 242 and 25 Hz); ^{19}F NMR (282 MHz, 17% (w/w) CD_3COCD_3) δ −121.4 and −121.5 (partial resolution, 6F), −123.55 (2F).

F10-diol: mp 159 °C; ^{1}H NMR (300 MHz, 15% (w/w) CD_3COCD_3) δ 4.11 (t, J_{HF} = 14 Hz), 5.36 (s, OH); ^{13}C NMR (75.5 MHz, 15% (w/w) CD_3COCD_3) δ 59.9 (t, J_{CH} = 25 Hz), 111.4 (Tquint, J_{CF} = 241 and 32 Hz), 115.4, 116.6 (Tt, J_{CF} = 240 and 25 Hz); ^{19}F NMR (282 MHz, 17% (w/w) CD_3COCD_3) δ −121.4/-121.5/-121.6 (partial resolution, 8F), −123.11 (2F).

2,2,3,3,4,4-Hexafluoro-1,5-dicyanatopentane (F3Cy). To a three-neck 100 mL flask fitted with a stirring bar, thermometer, nitrogen inlet, and dropping funnel were added 6.00 g (28.3 mmol) of F3-diol and 50 mL of acetone. After dissolution, this mixture was cooled to 0 to -10 °C, and 6.48 g (61.1 mmol) of BrCN was added. This mixture was further cooled to −35 °C. A solution of 6.17 g (61.1 mmol) of triethylamine in 7 mL of CH_2Cl_2 was transferred to the dropping funnel and added dropwise to the rapidly stirred F3-diol−BrCN mixture over 25 min while a −35 to −30 °C reaction temperature was maintained. The resulting suspension was stirred for 1 h at this temperature. The ice bath was removed, and, when the temperature warmed to 10 °C, the suspension was rapidly filtered, followed by washing the ammonium bromide salt with 10 mL of CH_2Cl_2. The combined filtrate and wash were extracted twice with 50 mL of distilled water and dried over anhydrous Na_2SO_4. Filtering and vacuum rotary evaporation yielded 9.25 g of an amber oil. IR indicated significant quantities of the diethylcyanamide byproduct present.[11] The product was vacuum distilled in a Kugelrohr apparatus (80 °C/0.025 Torr), yielding 4.64 g (63%) of colorless liquid product. Also collected was a 1.09 g fraction (30−60 °C/0.025 Torr) of diethylcyanamide, and ∼4 g of polymerized residue remained in the distillation flask. Characterization: mp −8 °C; ^{1}H NMR (300 MHz, 21% (w/w) CD_3COCD_3) δ 5.37 (t, J_{HF} = 13.9 Hz); ^{13}C NMR (75.5 MHz, 21% (w/w) CD_3COCD_3) δ 73.4 (t, J_{CH} = 27.6 Hz), 111.7 (−OCN), 110.8 (Tquint, J_{CF} = 261 and 28 Hz), 114.2 (Tt, J_{CF} = 259 and 32 Hz); ^{19}F NMR (282 MHz, 21% (w/w) CD_3COCD_3) δ −120.45 (2F), −124.63 (1F); IR (neat) ν 3042 (w, CH_2), 2987 (w, CH_2), 2266 (s, OCN), 1450 (w, CH_2), 1166 (s, CF_2), 1121 (s, CF_2) cm^{-1}. Anal. Calcd for $C_7H_4F_6N_2O_2$: C, 32.08; H, 1.54. Found: C, 31.99; H, 1.59.

2,2,3,3,4,4,5,5-Octafluoro-1,6-dicyanatohexane (F4Cy). To a three-neck 250 mL flask fitted with a stirring bar, thermometer, nitrogen inlet, and dropping funnel were added 10.00 g (38.2 mmol) of F4-diol and 50 mL of acetone. After dissolution, this mixture was cooled to 0 to −10 °C, and 8.90 g (84.0 mmol) of BrCN was added. This mixture was further cooled to −35 °C. A solution of 7.80 g (77.2 mmol) of triethylamine in 10 mL of acetone was transferred to the dropping funnel and added dropwise to the rapidly stirred F4-diol−BrCN mixture over 1 h while a −35 to −30 °C reaction temperature was maintained. The resulting suspension was stirred for 2 h at this temperature. The ice bath was removed, and, when the temperature warmed to 10 °C, the suspension was rapidly filtered, followed by washing the ammonium bromide salt with 10 mL of acetone. The combined filtrate and wash were concentrated by rotary evaporation. The amber oil was taken up into 50 mL of $CHCl_3$, extracted three times with 50 mL of distilled water and dried over anhydrous Na_2SO_4. Filtering and vacuum rotary evaporation yielded 15 g of an amber oil. The product was vacuum distilled in a

Kugelrohr apparatus (80 °C/0.025 Torr), yielding 6.76 g (57%) of colorless liquid product. Also collected was a 4.5 g fraction (30−60 °C/0.025 Torr) of diethylcyanamide, and ∼5 g of polymerized residue remained in the distillation flask. Characterization: MP 15 °C; ^{1}H NMR (300 MHz, 20% (w/w) CD_3COCD_3) δ 5.40 (t, J_{HF} = 13.1 Hz); ^{13}C NMR (75.5 MHz, 20% (w/w) CD_3COCD_3) δ 73.4 (t, J_{CH} = 27.4 Hz), 111.8 (−OCN), 111.1 (Tquint, J_{CF} = 265 and 31 Hz), 114.4 (Tt, J_{CF} = 269 and 31 Hz); ^{19}F NMR (282 MHz, 20% (w/w) CD_3COCD_3) δ −120.28 (2F), −122.95 (2F); IR (neat) ν 3043 (w, CH_2), 2986 (w, CH_2), 2266 (s, OCN), 1450 (w, CH_2), 1180 (s, CF_2), 1123 (s, CF_2) cm^{-1}. Anal. Calcd for $C_8H_4F_8N_2O_2$: C, 30.79; H, 1.29. Found: C, 30.60; H, 1.38.

2,2,3,3,4,4,5,5,6,6,7,7-Dodecafluoro-1,8-dicyanatooctane (F6Cy). To a three-neck 200 mL flask fitted with an overhead stirrer, thermometer, nitrogen inlet and dropping funnel was added 75 mL of acetone. After the acetone was cooled to −10 °C, 12.30 g (116 mmol) of BrCN was added, and the solution was cooled to −30 °C. A solution of 20.00 g (55.2 mmol) of F6-diol and 11.16 g (110.5 mmol) of triethylamine in 25 mL of acetone was prepared, transferred to the dropping funnel, and added dropwise with rapid stirring over a 40 min period while a −30 ± 5 °C reaction temperature was maintained. When the mixture had warmed to −5 °C, it was rapidly filtered, and the ammonium bromide salt was washed with 25 mL of acetone. The combined filtrate and wash was diluted with 100 mL of cold (−20 °C) CH_2Cl_2 and rapidly extracted with 100 mL of cold distilled water and two times with 100 mL of cold 1% NaCl. The CH_2Cl_2 phase was dried over anhydrous Na_2CO_3. Filtering and vacuum rotary evaporation yielded 21.61 g of a solid amber mass. This product was twice recrystallized from cold 2-propanol to yield 11.16 g (49%) of colorless crystalline product: mp 109 °C; ^{1}H NMR (300 MHz, 17% (w/w) CD_3COCD_3) δ 5.46 (t, J_{HF} = 13.1 Hz); ^{13}C NMR (75.5 MHz, 17% (w/w) CD_3COCD_3) δ 73.6 (t, J_{CH} = 26.7 Hz), 111.9 (−OCN), 111.5 (Tquint, J_{CF} = 262 and 29 Hz), 115.0 (Tt, J_{CF} = 260 and 33 Hz); ^{19}F NMR (282 MHz, 17% (w/w) CD_3COCD_3) δ −120.10 (2F), −121.55 (2F), −122.61 (2F); IR (neat) ν 3044 (w, CH_2), 2984 (w, CH_2), 2265 (s, OCN), 1450 (w, CH_2), 1196 (s, CF_2), 1143 (s, CF_2) cm^{-1}. Anal. Calcd for $C_{10}H_4F_{12}N_2O_2$: C, 29.14; H, 0.98 Found: C, 29.08; H, 1.06.

2,2,3,3,4,4,5,5,6,6,7,7,8,8,9,9-Hexadecafluoro-1,10-dicyanatodecane (F8Cy). To a three-neck 250 mL flask fitted with an overhead stirrer, thermometer, nitrogen inlet, and dropping funnel was added 90 mL of acetone. After the acetone was cooled to −25 °C, 9.43 g (89.0 mmol) of BrCN was added. A solution of 19.57 g (42.4 mmol) of F8-diol and 8.56 g (84.7 mmol) of triethylamine in 35 mL of acetone was prepared, transferred to the dropping funnel, and added dropwise with rapid stirring over a 45 min period while a −30 ± 5 °C reaction temperature was maintained. When the mixture had warmed to −5 °C, it was rapidly filtered, and the ammonium bromide salt was washed with 25 mL of acetone. The combined filtrate and wash was diluted with 125 mL of cold (˚20 °C) CH_2Cl_2 and rapidly extracted once with 100 mL of cold distilled water and two times with 100 mL of cold 1% NaCl. The CH_2Cl_2 phase dried over anhydrous Na_2CO_3. Filtering and vacuum rotary evaporation yielded 16.04 g of a solid amber mass. This product was recrystallized from a cold 1:7.5 acetone/2-propanol solvent mixture to yield 9.35 g (43%) of colorless crystalline product: mp 152 °C. ^{1}H NMR (300 MHz, 15% (w/w) CD_3COCD_3) δ 5.47 (t, J_{HF} = 13.1 Hz); ^{13}C NMR (75.5 MHz, 15% (w/w) CD_3COCD_3) δ 73.5 (t, J_{CH} = 26.8 Hz), 111.9 (−OCN), 111.6 (Tquint, J_{CF} = 263 and 30 Hz), 115.0 (Tt, J_{CF} = 260 and 33 Hz); ^{19}F NMR (282 MHz, 15% (w/w) CD_3COCD_3) δ −120.08 (2F), −121.37 (4F), −122.54 (2F); IR (neat) ν 3044 (w, CH_2), 2983 (w, CH_2), 2264 (s, OCN), 1450 (w, CH_2), 1201 (s, CF_2), 1147 (s, CF_2) cm^{-1}. Anal. Calcd for $C_{12}H_4F_{16}N_2O_2$: C, 28.14; H, 0.79 Found: C, 28.05; H, 0.88.

2,2,3,3,4,4,5,5,6,6,7,7,8,8,9,9,10,10,11,11-Eicosafluoro-1,10-dicyanatododecane (F10Cy). To a three-neck 250 mL flask fitted with an overhead stirrer, thermometer, nitrogen inlet, and dropping funnel was added 90 mL of acetone. After the acetone was cooled to −25 °C, 7.88 g (74.4 mmol) of BrCN was added. A solution of 19.91 g (35.4 mmol) of F10-diol and 7.16 g (70.8 mmol) of triethylamine in 35 mL of acetone was prepared, transferred to the dropping funnel, and added dropwise with rapid stirring over a 35 min period while a −30 ± 5 °C reaction temperature was maintained. When the mixture had warmed to −5 °C, it was rapidly filtered, and the ammonium bromide salt was washed with 125 mL of cold acetone (solubility was insufficient to use CH_2Cl_2 or $CHCl_3$). Na_2CO_3 drying and vacuum rotary evaporation yielded 18 g of a solid amber solid. This product was suspended with rapid stirring in 2-propanol to produce a fine suspension, which was filtered to yield 8.23 g of colorless crystalline solid product. Crystallization by cooling the filtrate produced an additional 1.71 g of product, and a final 6 g of very impure product was collected by evaporation. DSC and spectroscopic analyses indicated that the initial 8.23 g fraction was of particularly good purity, and it was used as prepared for subsequent experiments. Characterization: mp 181 °C; ^{1}H NMR (300 MHz, 15% (w/w) CD_3COCD_3) δ 5.47 (t, J_{HF} = 13.1 Hz); ^{13}C NMR (75.5 MHz, 15% (w/w) CD_3COCD_3) δ 73.5 (t, J_{CH} = 26.7 Hz), 111.9 (−OCN), 111.6 (Tquint, J_{CF} = 263 and 29 Hz), 115.0 (Tt, J_{CF} = 260 and 33 Hz); ^{19}F NMR (282 MHz, 15% (w/w) CD_3COCD_3) δ −120.02 (2F), −121.18 (6F), −122.48 (2F); IR (neat) ν 3044 (w, CH_2), 2984 (w, CH_2), 2264 (s, OCN), 1450 (w, CH_2), 1204 (s, CF_2), 1150 (s, CF_2) cm^{-1}. Anal. Calcd for $C_{14}H_4F_{20}N_2O_2$: C, 27.47; H, 0.66 Found: C, 27.29; H, 0.74.

Resin Cure Procedure. Prior to curing, the F3Cy and F4Cy monomers were degassed at 25 °C/1 Torr, and the F6Cy, F8Cy, and F10Cy monomers were degassed just above their respective melting points at 10 Torr vacuum. Monomers were thermally cured without added catalyst according to the schedule 125 °C/2 h → 175 °C/4 h → 225 °C/2 h, except for the F8Cy and F10Cy monomers, where the thermal cure schedule was initiated just above their melting points. The AroCy B and AroCy F monomers were degassed at 125 °C/1 Torr and thermally cured without added catalysts according to the schedule 125 °C/2 h → 175 °C/8 h → 260 °C/1.5 h.

Results

Monomer Synthesis. The synthesis of the NCO−$CH_2(CF_2)_nCH_2$−OCN (n = 3,4,6,8,10) monomer series proceeds by triethylamine-catalyzed reaction of the corresponding diol with ClCN or BrCN according to the method of Grigat and Pütter[2] (Figure 2). However, isolation of a pure monomer from unreacted reagents and byproducts is a critical issue. In addition to being undesirable contaminants, they have the deleterious effect of promoting the cyanate curing reaction at low temperatures. In some cases, this occurs at and below the melting point of the monomer, which is detrimental to processing operations. The presence of these catalytic impurities also causes significant losses in yield during purification as well as storage stability problems. The impurities (see Figure 2) include unreacted fluoro alcohol, triethylamine, the ammonium bromide salt, diethylcyanamide (von Braun side reaction product),

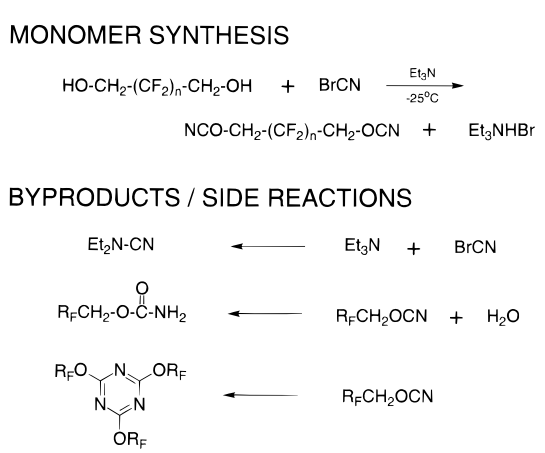

Figure 2. F*n*Cy monomer synthesis and side reactions.

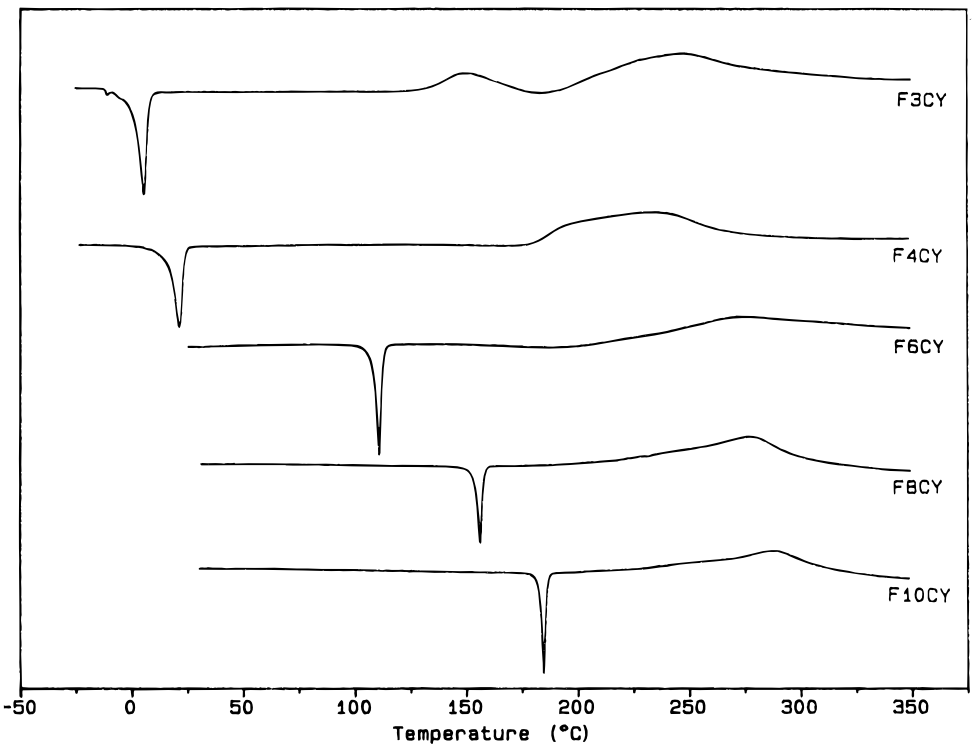

Figure 3. F*n*Cy monomer series DSC thermograms dipicting the monomer melting points and processing window.

and carbamate (from cyanate hydrolysis) in addition to trimerized product. Once sufficiently purified, these monomers are stable compounds and can be handled and stored.

Our initial approach was to employ the Grigat and Pütter cyanation reaction conditions and focus on purification operations. However, the apparent reactivity of the cyanate group made attempts to use alumina or silica chromatographic adsorbents unsuccessful, and this resulted in only the elution of small quantities of hydrolyzed cyanate. Distillation was practicable for the F3Cy and F4Cy members of the series, but relatively low pressures (0.025 Torr) are necessary and large losses occurred due to polymerization in the heated distilland. These losses could be reduced by drying reagents and solvents and by ensuring total conversion of the fluoro alcohol with a larger excess of BrCN/triethylamine. This excess results in formation of a larger quantity of diethylcyanamide, which appears to be less strongly catalytic than the fluoro alcohol. With this technique, the F3Cy and F4Cy monomers could be isolated with sufficient purity for processing operations. The best diagnostic of sufficient purity is the temperature range or processing window between the melting endotherm and onset of the trimerization exotherm in the DSC thermogram. For impure monomers, the trimerization exotherm superimposes on the melting transition, and, as higher levels of purity are obtained, it advances to an onset temperature of 200 °C. DSC thermograms for the purified F*n*Cy monomer series are presented in Figure 3.

The F6Cy, F8Cy, and F10Cy monomers could not be distilled and required recrystallization. Initially, the recrystallization of F6Cy with dichloroethane proved very tedious and difficult and was unsuccessful with the F8Cy and F10Cy monomers, as indicated in a preliminary report.[11] It was subsequently found that significant improvements in achievable purification could be made by altering the order of reagent mixing in the synthesis reaction[12] and by utilizing 2-propanol as the recrystallization solvent. Prereacting the fluoro alcohol with a stoichiometric quantity of triethylamine and then adding this mixture to the cold BrCN produced a cleaner crude product, and most of the diethylcyanamide from the large excess of cyanating reagents was eliminated. The 2-propanol appears to have a strong affinity for the impurities that catalyze the trimerization. With this procedure, it was possible to obtain F6Cy, F8Cy, and F10Cy monomers with sufficient purity that neat resin castings could be made.

Monomer Characterization. The monomers were characterized by DSC, IR, and NMR spectroscopies, and carbon/hydrogen analysis. The fluorinated diol precursors were also characterized by DSC and IR and NMR spectroscopy with the object of determining the presence of any incomplete fluorination in the fluoromethylene sequence or loss of diol functionality. No evidence for such effects was found.

The DSC thermograms for the purified F*n*Cy monomer series are presented in Figure 3. The melting point progressively increases with fluoromethylene sequence length (see Table 1) and, beyond a sequence length of 6 units, exceeds that of the corresponding alcohol (see experimental section). The exotherm is derived from the cyanate trimerization reaction and spans the range of 200−350 °C when monomers are sufficiently pure. As indicated above, the temperature range separating the melting transition and the onset of the curing exothermic transition defines the processing window and is an important diagnostic of operational purity.

The IR spectra of the F*n*Cy monomer series are presented in Figure 4. The spectra display bands characteristic of cyanate (O−C≡N stretch, 2265 cm^{-1}), fluoromethylene (CF_2, 1210−1120 cm^{-1}) and methylene (CH_2, 3040, 2980, 1450 cm^{-1}). Consistent with aliphatic cyanates, the cyanate band is not split by a Fermi resonance as occurs in aromatic cyanates.[13] As the fluoromethylene sequence length increases, the intensities of the O−C≡N and CH_2 bands diminish relative to those of the CF_2 bands. The corresponding wavenumber

Table 1. F*n*Cy Monomer Melting Point, IR, and NMR Spectroscopic Characterization[a]

		IR						NMR			
monomer	MP(°C)	ν_{CH_2}	ν_{CH_2}	ν_{CH_2}	ν_{OCN}	ν_{CF_2}	ν_{CF_2}	$\delta_{C\underline{H}_2}$	$\delta_{\underline{C}H_2}$	$\delta_{O\underline{C}N}$	$\delta_{C\underline{F}_2}$
F3Cy	−8	3042	2987	1450	2266	1166	1121	5.37	73.4	111.7	−120.45
F4Cy	15	3043	2986	1450	2266	1180	1123	5.40	73.4	111.8	−120.28
F6Cy	109	3044	2984	1448	2265	1196	1143	5.46	73.6	111.9	−120.10
F8Cy	152	3044	2983	1448	2264	1201	1147	5.47	73.5	111.9	−120.08
F10Cy	181	3044	2984	1448	2264	1204	1150	5.47	73.5	111.9	−120.02

[a] ν, IR band (cm^{-1}); δ, NMR chemical shift (ppm); $\delta_{C\underline{F}_2}$. resonance of terminal CF_2 unit.

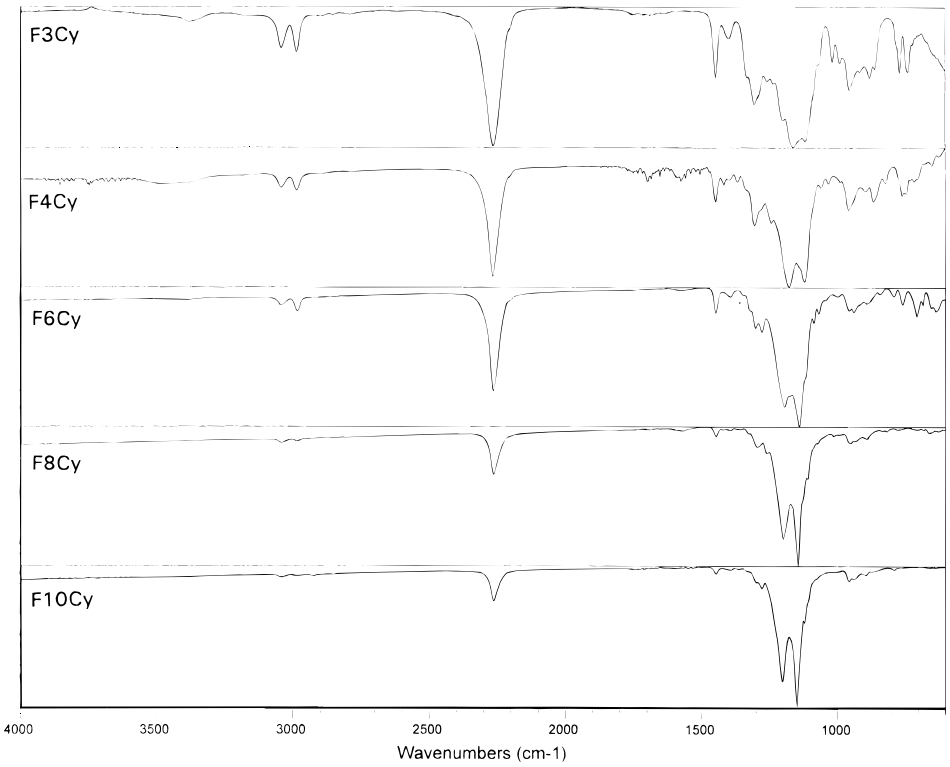

Figure 4. IR spectra of F*n*Cy monomer series.

shifts are presented in Table 1. As would be expected, most of the shifting occurs in the CF_2 bands, but both the O—C≡N and CH_2 bands exhibit a small wavenumber dependence on the CF_2 chain length.

The ^1H, ^{13}C, and ^{19}F NMR spectra of the F*n*Cy monomer series are consistent with the assigned structures. Chemical shift data of resonances assigned to the methylene protons, the cyanate and methylene carbons, and the terminal fluorines on the fluoromethylene sequence are presented in Table 1. The ^1H and ^{13}C resonances are triplets, with a small chemical shift dependence on fluoromethylene sequence length. The cyanate carbon resonance is at a slightly greater chemical shift than the 109 ppm generally observed for aromatic cyanates.[13] The ^{19}F spectra of the F*n*Cy monomer series are displayed in Figure 5. The terminal CF_2 resonance at −120.5 to −120.0 ppm is totally resolved from the internal CF_2 resonances and displays partially resolved fine structure and a small but regular dependence on fluoromethylene sequence length. This resonance is also sensitive to reaction of the cyanate group and very useful for the detection and identification of impurities such as unreacted alcohol, carbamate, and cyanurate. The second CF_2 resonance is the one shifted farthest upfield and also displays partially resolved fine structure and a stronger dependence on fluoromethylene sequence length. Resonances from CF_2 units 3 or more units inward from the terminal CF_2 unit are resolved from the first and second CF_2 resonances but begin to overlap each other, as indicated in the spectra of F6Cy, F8Cy, and F10Cy monomers.

Polymerization. It is well established by a variety of techniques that aromatic cyanate esters cyclotrimerize to form cross-linked cyanurate networks.[12] Analogously, the fluoromethylene cyanate monomers thermally cure to cyanurate networks. Typically, monomers are advanced to prepolymers by thermal treatment at 120 °C or just above the melting point and then cured at 175 °C and postcured at 225 °C. Both NMR and infrared spectroscopies exhibit features indicating formation of the cyanurate linkage as the cyanate functional group is consumed. In the ^{13}C NMR spectra, a new resonance appears at 173.6 ppm and is assigned to the carbon in the cyanurate heterocycle.[12,13] Coincident with this conversion is the appearance and growth of methylene ^{13}C and ^1H triplet resonances shifted upfield 9.4 and 0.21 ppm, respectively, from those of the monomer. In the ^{19}F spectrum, the terminal fluoromethylene group shifts upfield 1.13 ppm as a result of the conversion and is particularly useful for quantifying it (see Figure 6). In the IR spectrum, new bands appear at 1580 and 1370 cm^{-1}, characteristic of the triazine ring in the cyanurate structure with a coincident decline in the 2265 cm^{-1} O—C≡N band.[14] The area of the O—C≡N band relative to the area of the CH_2 bands (3044 and 2985 cm^{-1}) is a convenient measure of cure at high conversions. Infrared analysis of casting prepared for resin property measurements in this study

Table 2. F*n*Cy and AroCy F Resin Physical Property Characteraction[a]

resin	% F	ρ (g/cm^3)	γ_c (dyn/cm)	n_D^{25}	ϵ' dry (1.0 GHz)	tan δ (1.0 GHz)	% H_2O absorption	ϵ' wet (1.0 GHz)
F3Cy	43.5	1.771	40	1.447	2.66	0.021	1.67	3.31
F4Cy	48.7	1.814	36	1.433	2.50	0.018	0.93	2.73
F6Cy	55.3	1.856	31	1.408	2.29	0.018	0.75	2.62
F8Cy	59.4	1.889	27	1.395	2.32	0.016	0.74	
F10Cy	62.1	1.908	23	1.382	2.31	0.017	0.68	
AroCy F	29.4	1.471	40	1.532	2.54	0.007	1.61	2.82

[a] ρ, density at 25 °C; γ_c, critical surface tension; n_D^{25}, refractive index at 589 nm and 25 °C; ϵ', dielectric constant; % H_2O absorption; 100 °C immersion/96 h; ϵ' wet, dielectric constant of a casting treated by 100 °C water immersion/96 h and stored at 23 °C immersed in water.

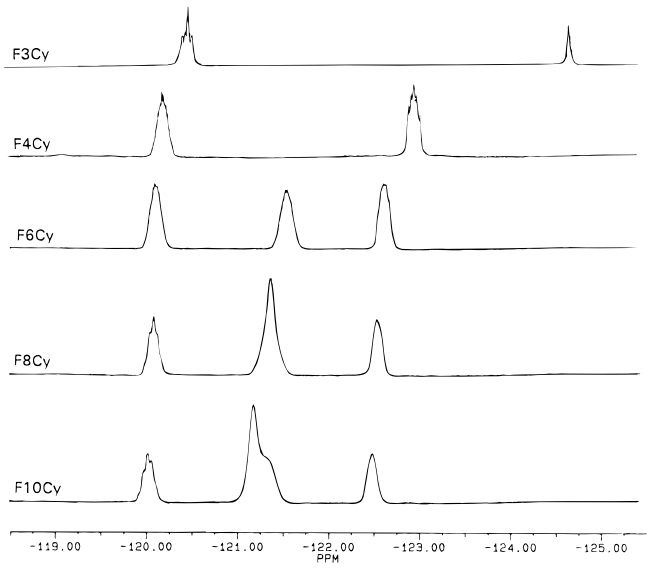

Figure 5. ^{19}F NMR spectra of F*n*Cy monomer series.

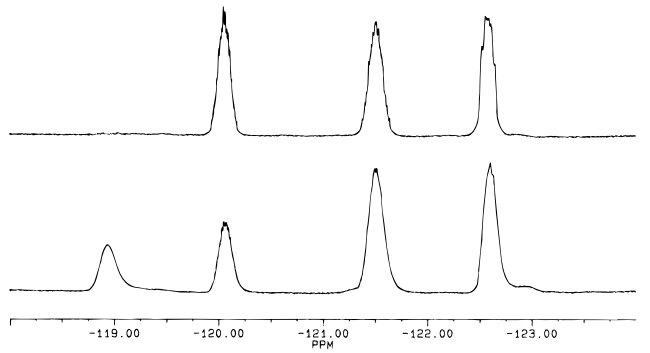

Figure 6. ^{19}F NMR spectra showing the effect of cyanurate formation on the terminal CF_2 resonance. (TOP) F6Cy monomer and (bottom) at a 42% conversion to cyanurate.

indicated that the conversion of cyanate is relatively high, ranging from 94 to 99%. In comparison with aromatic cyanates,[12] these high conversions without the use of transition metal accelerators are probably a consequence of the low glass transition temperatures of the F*n*Cy system.

Castings of neat resin, prepared as described above, are clear amber in appearance and are cut to dimensions appropriate for the various characterizations.

F*n*Cy Resin Properties. Tables 2 and 3 summarize the properties of cured resin castings of the F*n*Cy system and of AroCy F. AroCy F is the fluorinated aromatic cyanate resin based on the dicyanate of 6F-bisphenol A and is included as a relevant reference for comparison.

The second column in Table 2 is the fluorine content. It is based on the fluorine content of the corresponding

Table 3. F*n*Cy and AroCy F Resin Thermal Characteraction[a]

resin	T_g (°C)	α_G (ppm/°C)	α_R (ppm/°C)	$T_{10\%d}$ (°C)	$(\Delta m/\Delta t)_{300°C}$ (%/min)
F3Cy	86	109	238	440	−0.0196
F4Cy	84	124	244	448	−0.0191
F6Cy	92	144	248	450	−0.0156
F8C	92	145	255	471	−0.0133
F10Cy	101	152	275	479	−0.0064
AroCy F	256	65.9	223	461	−0.0024

[a] α_G, glassy state thermal expansion coefficient; α_R, rubbery state thermal expansion coefficient; $T_{10\%d}$, temperature at 10% weight loss; $(\Delta m/\Delta t)_{300°C}$, percent weight loss per minute at 300 °C.

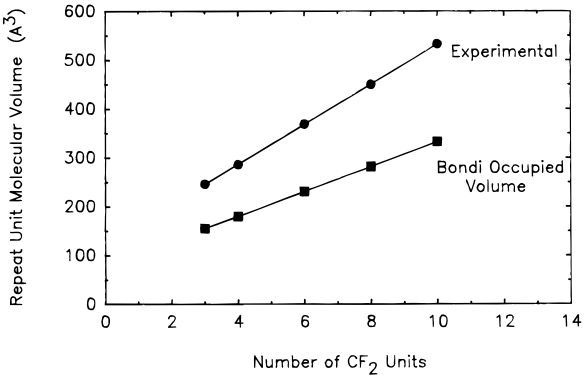

Figure 7. Effect of increasing fluoromethylene chain length on the F*n*Cy repeat unit molecular volume. The experimental value was calculated from the density measurements. The Bondi occupied volume is calculated from the van der Waal volume parameters (see text).

monomer and reflects the composition as a function of the fluoromethylene sequence length. The third column is the density measurement for the series of resins. This measurement parallels that of the fluorine content, as would be expected. The F*n*Cy resin system is a $(CF_2)_n$ homologous series, with the molecular volume of the repeat unit increasing by integral numbers of CF_2 units. In Figure 7, a plot of this quantity (calculated from the density) against the number of fluoromethylene units in the sequence shows a linear dependence, with a slope of 41.0 Å^3/CF_2 unit. This is in good agreement with an analogous value of 41.5 Å^3/CF_2 unit calculated from the PTFE repeat unit molecular weight (50 g/mol) and amorphous density (2.0 g/cm^3).[15]

The critical surface tension for wetting of the F*n*Cy, AroCy F, and AroCy B resins was determined from contact angle measurements of water, formamide, methylene iodide, *o*-tricresyl phosphate, and dicyclohexyl deposited on clean, flat resin surfaces. The Zisman wettability plot of contact angle cosine as a function of liquid surface tension is presented in Figure 8. Analysis based on a linear dependence yields the critical surface tension for wetting for each resin reported in Table 2.

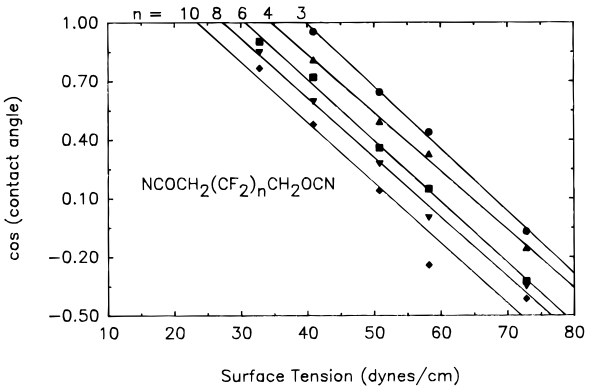

Figure 8. Zisman plot of the F*n*Cy resin series. The value of *n* is indicated at the top of the plot.

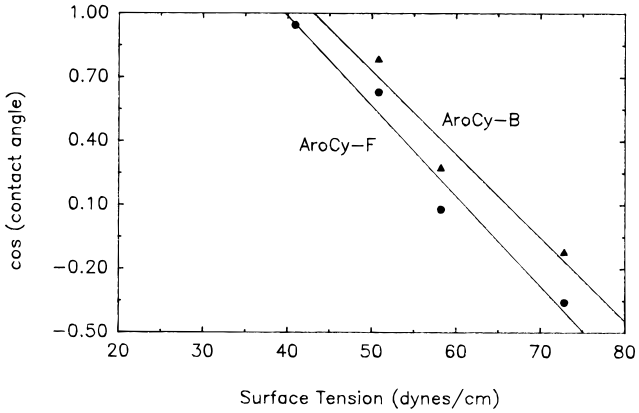

Figure 9. Zisman plot of the AroCy F and AroCy B resins.

For the F*n*Cy series, this result parallels the fluoromethylene sequence length in the resin structures and, on the basis of fluorine content, begins to approach a value close to that of the 18 dyn/cm characteristic of PTFE. The Arocy resins exhibit higher critical surface tensions as well as larger slopes in the Zisman plot (See Figure 9). The larger slope correlates with a larger surface solubility of spreading liquids in the resin[16] and may be indicative of a lower packing efficiency in the AroCy resins.

The refractive index was measured at 589 nm on polished surfaces of the F*n*Cy and AroCy F castings (Table 2). The F*n*Cy resins display a progressively decreasing refractive index with increasing fluorine content, which would be expected from the lower polarizibility of the fluorine atom. At a fluoromethylene sequence length of 10 units, the F10Cy refractive index is significantly above that (1.293) calculated for amorphous PTFE but is approaching those of other highly fluorinated aliphatic polymers.[17] The presence of the aromatic cyanurate linkage and the CF_2CH_2 junction represents polarizable structures that contribute to higher refractive indexes. The AroCy F result reflects the effect of the aromatic structures.

Complex electric field permittivity was measured on F*n*Cy and AroCy F castings as a function of frequency over a range of 500−1500 MHz. Plots of the dielectric constant, ϵ', and loss tangent, tan δ, as a function of frequency are presented in Figures 10 and 11 for the resins in the dry state. Data for PTFE have been included as a reference. Previous AroCy F dielectric constant measurements of 2.5[7,18] are in agreement with the result of this study. The F*n*Cy resins have a gradual decrease in dielectric constant with increasing frequency, characteristic of a dipole orientation polarization effect. The AroCy F resin has dielectric constant intermediate between the F3Cy and F4Cy resins. As the fluoromethylene sequence length of the F*n*Cy resin series increases to 6 units, the dielectric constant decreases to 2.3. Increasing the sequence length to 8 or 10 CF_2 units does not result in lower dielectric constants or those that might approach the 2.0 limit represented by PTFE. This truncation of the dielectric constant at 2.3 indicates that effects other than an electronic polarizability associated with fluorine content are major determinants. The tan δ dependence on frequency displays a gradual decrease with increasing frequency which is similar to that of the dielectric constant. The AroCy F resin has a significantly lower tan δ than the F*n*Cy series. The tan δ is a measure of stored electromagnetic energy that is lost as heat dissipation, and it correlates with molecular relaxation mechanisms. The F*n*Cy resins have a T_g that is approximately 150 °C below that of AroCy F (see Table 3). This difference permits a more facile molecular relaxation and correlates with the larger tan δ of the F*n*Cy resins. Within the F*n*Cy series, tan δ decreases with increasing fluoromethylene sequence length, the effect of which becomes larger at higher frequencies. However, the 0.0002 limit of PTFE is not closely approached, which is reasonable considering the high crystallinity and absence of dipoles in PTFE.

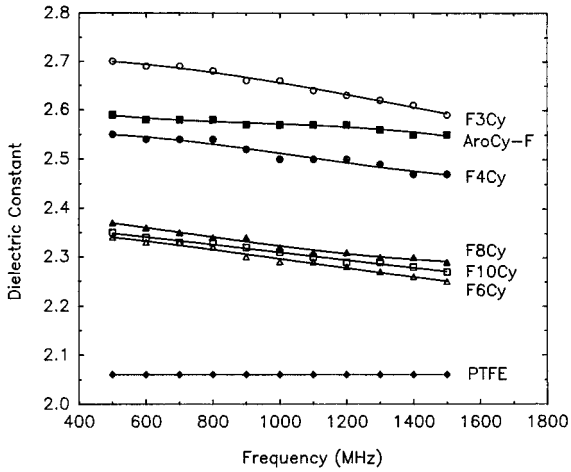

Figure 10. Dielectric constant dependence on frequency for F*n*Cy, AroCy F, and polytetrafluoroethylene resins.

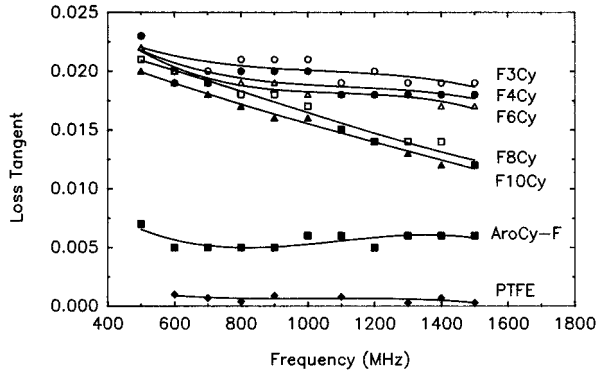

Figure 11. Loss tangent dependence on frequency for F*n*Cy, AroCy F and polytetrafluoroethylene resins.

Hydrophobicity or moisture absorption was measured by immersing castings of the F*n*Cy and AroCy F resins in 100 °C distilled water. This moisture absorption as a function of time is plotted in Figure 12. An equilibrium moisture adsorption is more rapidly attained by the F*n*Cy resin series compared with the AroCy F

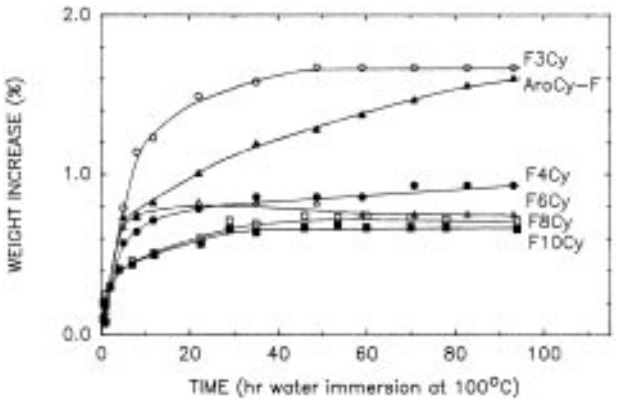

Figure 12. Water absorption (100 °C immersion) of F*n*Cy and AroCy F resins.

system. This may be a consequence of a large difference in T_g. The T_g ranges from 80 to 100 °C for the F*n*Cy resins and is 256 °C for the AroCy F resin (see below). In the F*n*Cy series, moisture absorption decreases as the fluoromethylene sequence length progresses to 6 units, and then it remains nearly constant at 0.7 wt % with the increment to 8 and 10 CF_2 units. This is similar to the trend observed with the dielectric constant. The moisture absorption also elevates the dielectric constant. The dielectric constants of castings subjected to this immersed boiling water treatment are presented in Table 2. As expected, absorption of water increases the dielectric constant. A quantitative correlation of the amount of water absorbed with the increment in dielectric constant will require an experiment designed to study castings with variable and uniformly distributed water contents.

Thermal analyses of the F*n*Cy and AroCy F resins included DSC, TMA, and TGA. The glass transition was relatively weak and somewhat difficult to measure by DSC. Using 20−30 mg samples improved the sensitivity, but the transition was still relatively broad (see Figure 13). The TMA thermograms define a narrower T_g temperature range and provide glassy and rubbery state thermal expansion coefficients (α_G and α_R, respectively) as well. The TMA thermogram of F10Cy as depicted in Figure 14 is typical, and the respective T_g, α_G, and α_R data for the F*n*Cy series and AroCy F resins are presented in Table 3. The glass transitions of the F*n*Cy series fall within a 10−20 °C range, gradually increasing with the CF_2 sequence length. The AroCy F T_g is in agreement with the 265 °C previously reported.[18] The thermal expansion coefficients of the F*n*Cy series, particularly α_G, are significantly larger than those for AroCy F. This is large for a thermoset and is attributed to the fluoroaliphatic character of the F*n*Cy system. Also, within the F*n*Cy system, there is a correlation of increasing thermal expansion coefficient with increasing fluoromethylene sequence length and, consequently, decreasing cross-link density.

Thermal stability was assessed by TGA. In common with most cyanate ester resins,[19] scanning TGA of the F*n*Cy resins shows a catastrophic weight loss in the 410−430 °C temperature range. The F10Cy thermogram in Figure 15 is typical. As a crude index of thermal stability, the temperature corresponding to 10% weight loss is entered in Table 3 for the F*n*Cy and AroCy F resins. The scanning TGA grossly overestimates thermal stability. Isothermal TGA is more effective in discriminating thermogravimetric stability between materials as well as more useful in screening materials for practical applications. It is proposed to use an inert atmosphere 300 °C isothermal measurement of the rate of weight loss. This measurement is taken as the slope of a straight line approximation between the 20 min and 2 h points of an isothermal TGA thermogram. These data for the F*n*Cy and AroCy F resins are illustrated in Figure 16, and results are entered into Table 3 as $(\Delta m/\Delta t)_{300°C}$. This result shows that the aromatic AroCy F is more stable than the fluoroaliphatic F*n*Cy resins. Within the F*n*Cy series, the thermostability increases with increasing fluoromethylene sequence length. This runs contrary to cross-link density and indicates that the methylenecyanurate structural unit is the thermally less stable structural component.

Discussion

The key aspect of the F*n*Cy monomer synthesis is the purification. If not sufficiently purified, the monomer will not process or processing times will be too short for melt manipulation. Also, the monomer will not be stable for storage, and gel particles will be observed on remelting or redissolution. The DSC thermogram is the best indicator to determine whether catalytic impurities have been sufficiently removed. The cure reaction exotherm should be displaced to temperatures significantly higher than the monomer melting point, as indicated in Figure 3. In one isolated instance, a batch of F6Cy monomer was purified to an extent that monomer evaporation superimposed on the exotherm, and this particular batch did not gel after 4 h at 125 °C. This is an indication that highly purified monomer is stable toward the cyclotrimerization reaction and that a catalytic additive may, in such cases, be necessary. It is suspected that uncyanated alcohol is the most active of the catalytic impurities. An in-depth study discriminating the relative catalytic activities of the known impurities as well as the monomer hydrolytic susceptibility is in progress with the F6Cy system. Conditions which greatly facilitate the purification are to employ a presalting of the fluoro alcohol and amine reagents, to avoid any heating of the reaction mixture during workup, and to utilize 2-propanol in the recrystallization where appropriate. Within the F*n*Cy series, the F6Cy monomer has the most facile purification.

Because of the simplicity of monomer structure, the spectroscopic characterization is particularly facile. In this respect, ^{19}F NMR is particularly useful in that impurities and conversion by trimerization can be determined with little interference arising from solvents or other reagents.

The properties of the cured F*n*Cy resins display two trends with increasing fluoromethylene sequence length. The first trend is a continual increasing or decreasing property dependence on the number of CF_2 units. The density, critical surface tension, refractive index, glass transition, thermal expansion, and thermal stability follow this trend. The second trend is a limitation of the property at the CF_2 sequence length of 6 units. The dielectric constant (0.5−1.5 GHz) and boiling water absorption follow this trend.

The difference in trends for the refractive index and dielectric constant is puzzling. In the literature, the effects of fluorine substitution in polyimides on these two properties have been elegantly investigated,[20−22] and the insight is relevant to the F*n*Cy resins. The major contributing effects to the dielectric constant were shown to include electronic polarization, dipole orienta-

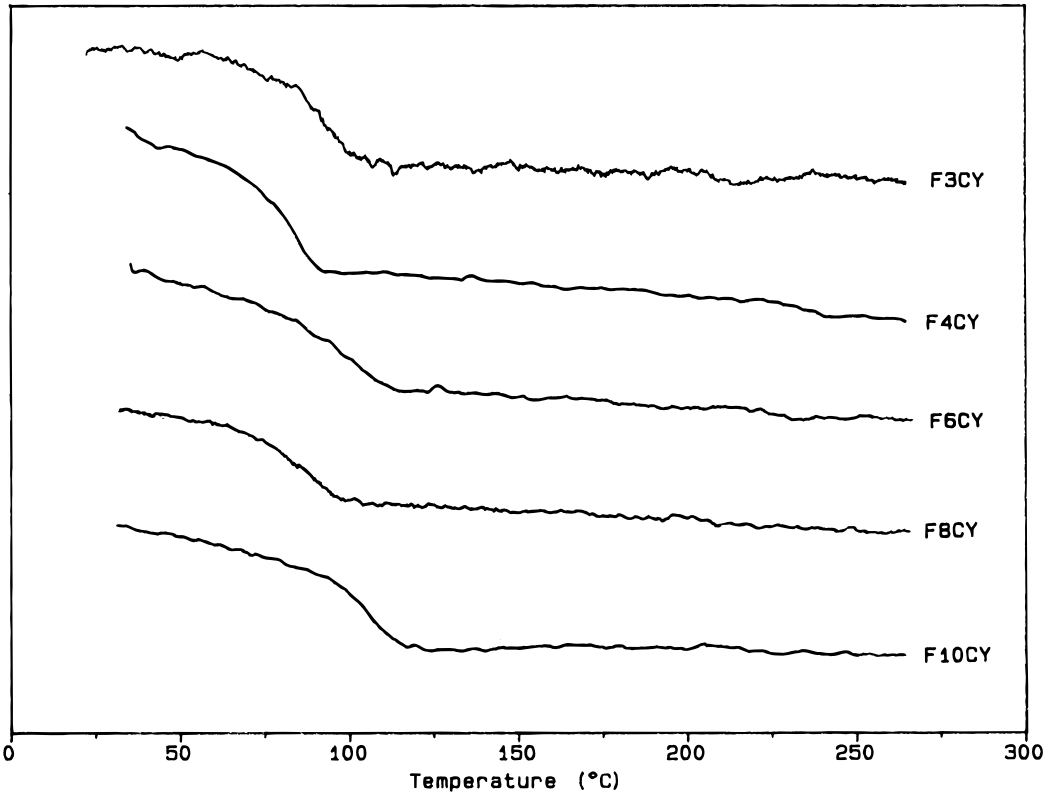

Figure 13. DSC thermograms of F*n*Cy resin series depicting the glass transition.

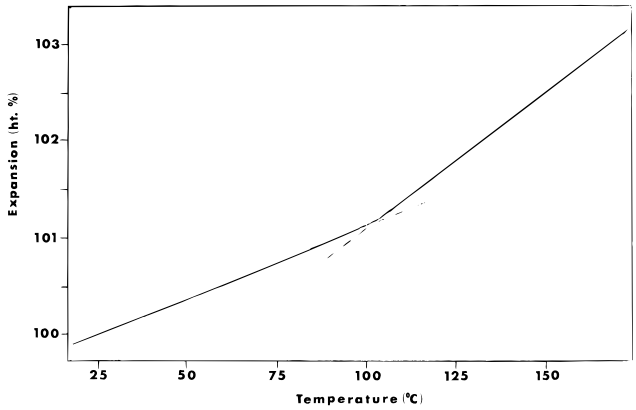

Figure 14. TMA thermogram of F10Cy cured resin.

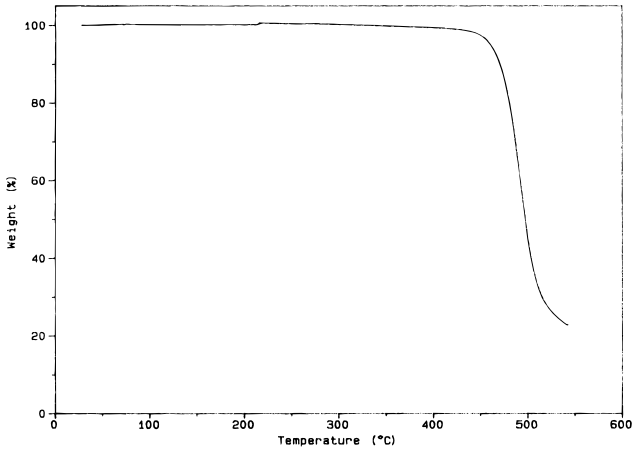

Figure 15. Scanning TGA thermogram of F10Cy cured resin.

tion polarization, free volume, and moisture absorption. Electronic polarization pertains to a very rapid electric field-induced distortion of electron density surrounding the nuclei at the molecular structure level. This response occurs at optical frequencies and is influenced by the polarizibility of the electrons associated with constituent atoms. Fluorine, being the least polarizable element, will lower this electronic polarization contribution to the dielectric constant when substituted for other elements. The Maxwell relation, equating this contribution to the square of the refractive index, has been used as a measure of this effect, assuming other contributors to be negligible at optical frequencies.[21] In Figure 17, this optical frequency dielectric constant (n^2) and the 1.0 GHz dielectric constant (ϵ') are plotted against the number of CF_2 units in the F*n*Cy resin series. Beyond a sequence length of 6 CF_2 units, the decrease in optical frequency dielectric constant is not paralleled by a decrease in the 1.0 GHz dielectric constant. Subtraction of the optical frequency dielectric constant from that measured at 1.0 GHz ($\epsilon' - n^2$) more clearly shows the effect of other contributors to the lower frequency dielectric constant.[23] At a CF_2 chain length greater than 6, these other factors increase the dielectric constant.

Dipole orientation polarization pertains to the conformational movement of the permanent dipoles responding to an electric field. In solids, the conformational freedom of the chemical structure responsible for the dipole is an important determinant of this effect. As reported for the polyimide system, the substitution of fluorine and its symmetry can generate appreciable dipoles which may significantly enhance the contribution of the dipole orientation effect to the dielectric constant.[21] This effect is more pronounced at lower frequencies and superimposes on the electronic polarization contribution to the dielectric constant. In the F*n*Cy system, the permanent dipoles should reside in the CF_2CH_2 junction and in the ether linkage between the methylene and triazine structures. The dipoles associated with these structures are significant and have conformational freedom.[24] However, with increas-

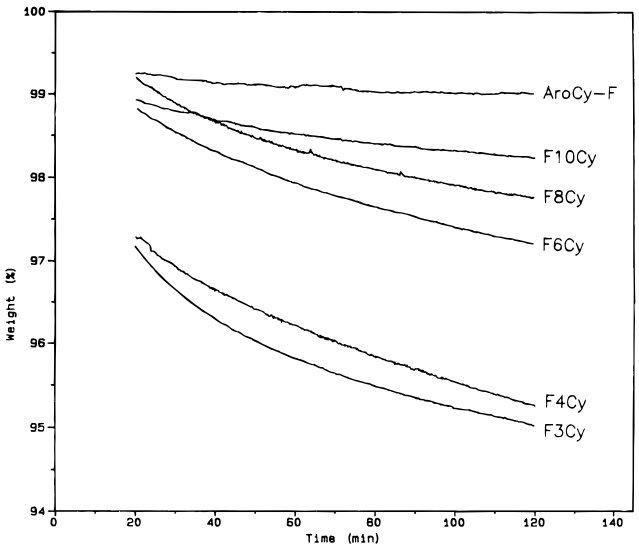

Figure 16. Isothermal (300 °C) TGA thermograms of F*n*Cy and AroCy F resins.

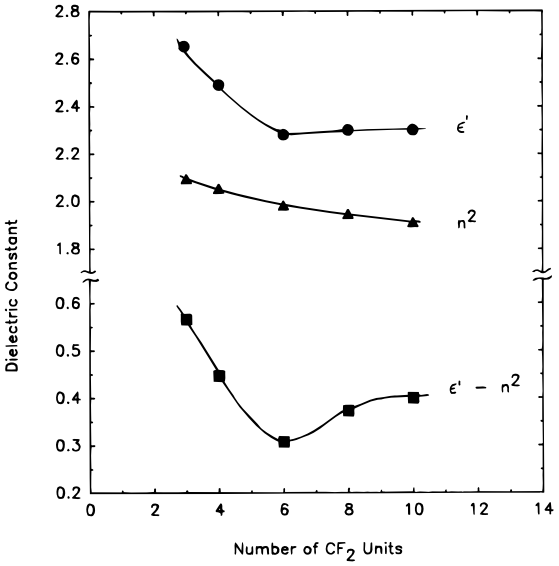

Figure 17. Dielectric constant dependence on CF_2 chain length. ϵ' is the 1.0 GHz dielectric constant; n^2 is the calculated optical frequency dielectric constant calculated from the refractive index measurement ($n_D^2 = 589$ nm, see text); and $\epsilon' - n^2$ is the 1.0 GHz measurement with the optical frequency component subtracted and represents dipole contributions to the dielectric constant.

ing fluoromethylene chain sequence length, the density of these dipoles should decrease with a corresponding drop in the dielectric constant. This was not observed.

It is possible to speculate that a dipole might actually be generated if the CF_2 chain in an amorphous matrix surpasses a length necessary to form a kink or bend. A dipole of 1.6 D oriented from the carbon nucleus to the midpoint between the fluorine nuclei is associated with an isolated CF_2 unit.[25] In the PTFE crystal structure, the CF_2 chain is in the low-energy trans conformation (offset by 17° due to steric repulsion of fluorine substituents), and the dipoles associated with adjacent CF_2 units cancel. However, the perfluoromethylene chain is not completely rigid, and, while it is much stiffer than the methylene chain, rotational isomerism imparts some flexibility to the CF_2 chain.[26] In the gauche conformation, dipoles associated with adjacent CF_2 units are oriented such that they do not cancel, and a net dipole from a sequence of CF_2 units in the gauche conformation might contribute to the measured dielectric constant. In the F*n*Cy resin series, the longer CF_2 sequences of the $n = 6$, 8, and 10 systems and progressively lower cross-link densities may increase the possibility of forming kinks, which may generate dipoles and contribute to the measured dielectric constant. This is a speculative proposition, and no references to experimental data correlating dielectric constant or dipole moment measurements with rotational isomerism of a CF_2 chain have been located.

Free volume has a strong role in lowering the dielectric constant by diluting the density of polarizable groups with void space. The free volume increment that accompanied fluorine substitution in polyimides has been shown to be very effective.[22] In the F*n*Cy resin system, if the packing efficiency were to increase once a threshold CF_2 chain length was exceeded, a free volume contribution to the dielectric constant would diminish, which might explain the deviation of the F8Cy and F10Cy resins from the experimental trend in the F3Cy through F6Cy resins. Longer CF_2 sequences and a lower cross-link density might facilitate this effect. To diagnose such an effect, it is possible to calculate an occupied volume for the molecular repeat unit using van der Waals radii volume equivalents of substructures derived by Bondi[28] and subsequently calculate the free volume fraction from the ratio of Bondi occupied volume to the experimental density-derived volume of the molecular repeat unit. The calculated occupied volumes of the molecular repeat unit of the F*n*Cy resin series[29] are presented in Figure 7. The corresponding fractional free volumes are 0.370, 0.371, 0.374, 0.373, and 0.375 for the respective F*n*Cy resins $n = 3$, 4, 6, 8, and 10. If the third decimal place is considered to be significant, this calculation shows a small trend. Small changes in calculated free volume fractions (on the order of 0.01−0.04) have been shown to correlate with measurable and significant changes in the dielectric constant (on the order of 0.09−0.14) in fluorinated polyimide systems.[22] However, for the F*n*Cy series, this variation in free volume fraction is smaller (on the order of 0.005), and the accuracy of the volume equivalents used for the calculation could be a factor. The magnitude of the variation in free volume fraction does not appear to indicate that significant enhancement in packing efficiency occurs at a sequence length of 6−10 fluoromethylene units.

Very large effects on the dielectric constant are caused by the absorption of moisture. The increments in dielectric constant (1 kHz) reported for the polyimide system caused by exposure to 40% humidity ranged from 0.41 to 0.17 as the fluorine content increased from 21 to 36%.[20] In the current work, precautions against humidity exposure between fabrication of the casting and the dry dielectric constant measurement involved desiccator storage. Following this measurement, the castings were repeatedly exposed to the ambient atmosphere over a period of several months. To check for the amount of moisture adsorbed and the reproducibility of the dielectric constant measurement, these castings were vacuum dried (135 °C/1 Torr/40 h) and remeasured. The weight lost, presumably moisture, ranged from 0.35 to 0.060% for the F*n*Cy resin series ($n = 3$−10) and was 0.52% for the AroCy F resin, but no change in dielectric constant relative to the initial measurement was observed.

In summary, the trend where the dielectric constant does not further decrease as the CF_2 sequence length

exceeds 6 is reproducible, but a physical cause is currently an issue of speculation.[30]

With respect to comparing the F*n*Cy resin properties to those of AroCy F, the results follow what would be expected in trading fluoroaliphatic character for aromatic character. The glass transition, refractive index, critical surface tension, dielectric constant, and water absorption are significantly lower, and the thermal expansion is higher. Thermogravimetric stability, contrary to expectation, is lower. A model compound report in the literature indicated that a fluoroaliphatic cyanurate is more thermally stable that an aromatic cyanurate.[31] The isothermal TGA result of this study indicates that the aromatic cyanate is the more thermally stable structure at 300 °C. Regarding electric field permittivity, the dielectric constant and tan δ of the F*n*Cy resins reflect a molecular structure having less polarizability but more conformational mobility than the AroCy F system.

The optimum trade-off between properties and processing for the F*n*Cy resins occurs at a fluoromethylene chain length of 6. The F6Cy monomer is the most facile to purify, has an acceptable processing window, and attains the minimal 2.3 dielectric constant of the series. Longer fluoromethylene sequences would only return a modest increase in T_g and a slight improvement in thermal stability. For the purpose of future evaluation on a larger scale, the F6Cy system will be examined for hydrolytic stability, catalytic susceptibility, prepolymer formation, mechanical properties, and dielectric thermal stability.

Summary

A series of fluoromethylene cyanate ester monomers ($N{\equiv}CO{-}CH_2(CF_2)_nCH_2{-}OC{\equiv}N$, n = 3, 4, 6, 8, and 10) have been synthesized and characterized. Melting points range from −8 to 181 °C, and characterization includes ^1H, ^{13}C, and ^{19}F NMR and IR spectroscopy and DSC. Purification is a critical requirement for melt processing. The thermal curing reaction is a cyclotrimerization reaction of the cyanate functional group to the cyanurate heterocycle. Physical properties of resin castings and their variation with increase in fluoromethylene sequence length from 3 to 10 include density, 1.77−1.91 g/cm^3; critical surface tension, 40−23 dyn/cm; refractive index, 1.447−1.382; dielectric constant, 2.6−2.3; 100 °C immersion water absorption, 1.67−0.68%; T_g, 84−101 °C; glass/rubber thermal expansion coefficient, 109/238−152/275 ppm/ °C; gravimetric thermal stability, 0.0196−0.0064% weight loss/min at 300 °C. Compared with aromatic cyanate ester resins, the fluoromethylene cyanate esters have significantly lower T_g, dielectric constant, critical surface tension, and water absorption. For low-dielectric applications, the optimum trade-off between properties and processing occurs at a fluoromethylene chain length of 6.

Acknowledgment. The authors gratefully acknowledge D. A. Shimp of Ciba Geigy for many very helpful discussions and the generous contribution of the AroCy F and AroCy B monomers, E. Grigat for helpful discussions and background, and the Office of Naval Research for financial support.

References and Notes

(1) Grigat, E.; Pütter, R. German Patent 1,195,764, 1963.
(2) Grigat, E.; Pütter, R. *Chem. Ber.* **1964**, *97*, 3012.
(3) (a) Martin, D. *Angew. Chem.* **1964**, *76*, 303. (b) Jensen, K. A.; Holm, A.; Thorkilsen, B. *Acta Chem. Scand.* **1964**, *23*, 1916.
(4) Jensen, K. A.; Due, M.; Holm, A.; Wentrup, C. *Acta Chem. Scand.* **1966**, *20*, 2091.
(5) Loudas, B. L.; Vogel,H. A. U.S. Patents 3,681,292, 1972; 3,733,349, 1973.
(6) Shimp, D. A. In *Chemistry and Technology of Cyanate Ester Resins*; Hamerton, I., Ed.; Chapman & Hall: Glasgow, 1994; Chapter 10, p 282.
(7) Shimp, D. A.; Chin, B. In *Chemistry and Technology of Cyanate Ester Resins*; Hamerton, I., Ed.; Chapman & Hall: Glasgow, 1994; Chapter 8, p 230.
(8) Mumby, S. J. *J. Elect. Mater.* **1989**, *18*, 241.
(9) Bussey, H. *Proc. IEEE* **1967**, *55 (6)*, 1046.
(10) Von Hippel, A. *Dielectrics and Waves*; Wiley: New York, 1954; p 4.
(11) Snow, A. W.; Buckley, L. J. *Proc. Am. Chem. Soc. Div. Polym. Mater.: Sci. Eng.*, **1996**, *74*, 55.
(12) Fang, T.; Shimp, D. A. In *Progress in Polymer Science*; Vogl, O., Ed.; Elsevier Science Ltd.: Oxford, 1995; Vol. 20, pp 61−118.
(13) Snow, A. W. In *Chemistry and Technology of Cyanate Ester Resins*; Hamerton, I., Ed.; Chapman & Hall: Glasgow, 1994; Chapter 2, p 7.
(14) Snow, A. W.; Buckley, L. J. *Proc. Am. Chem. Soc. Div. Polym. Mater.: Sci. Eng.*, **1995**, *72*, 439.
(15) Koo, G. P. In *Fluoropolymers*; Wall, L. A., Ed.; Wiley-Interscience: New York, 1972; p 513.
(16) Johnson, R. E., Jr.; Dettre, R. H. In *Wettabiltiy*; Berg, J. C., Ed.; Marcel Dekker, Inc.: New York, 1993; Chapter 1, p 1.
(17) Groh, W.; Zimmermann, A. *Macromolecules* **1994**, *27*, 5964.
(18) Shimp, D. A.; Christenson, J. R.; Ising, S. J. *Int. SAMPE Symp., 34th* **1989**, *34*, 222.
(19) Hamerton, I. In *Chemistry and Technology of Cyanate Ester Resins*; Hamerton, I., Ed.; Chapman & Hall: Glasgow, 1994; Chapter 7, p 193.
(20) Hougham, G.; Tesoro, G.; Shaw, J. *Macromolecules* **1994**, *27*, 3642.
(21) Hougham, G.; Tesoro, G.; Viehbeck, A.; Chapple-Sokol, J. D. *Macromolecules* **1994**, *27*, 5964.
(22) Hougham, G.; Tesoro, G.; Viehbeck, A. *Macromolecules* **1996**, *29*, 3453.
(23) The reviewer is gratefully acknowledged for this suggestion.
(24) A maximum dipole moment associated with a CF_2CH_2 junction is 2.1 D. This is derived from a vector addition of 1.6 D associated with an isolated CF_2 unit and 0.5 D associated with an isolated CH_2 unit bonded in the trans conformation.[25] The fluoromethylene chain connecting the terminal CF_2CH_2 dipoles is not a rigid rod in an all-trans conformation, but the energy of the gauche conformation as well as the energy of activation for the trans to gauche rotation is such that the fluoromethylene chain has a greater persistence of direction and a reduced flexibility relative to the methylene chain.[26] The dipole associated with the ether linkage should not be greater than the 1.38 D of anisole,[27] but perhaps more important is the ease of rotation around the ether linkage. While this conformational freedom has been acredited for the mechanical toughness of cyanate resins,[12] it is a facilitating mechanism for dipole orientation of both that associated with the ether linkage and the CF_2CH_2 junction.
(25) Peterlin, A.; Elwell, J. H. *J. Mater. Sci.* **1967**, *2*, 1.
(26) Bates, T. W. In *Fluoropolymers*; Wall, L. A., Ed.; Wiley-Interscience: New York, 1972; Chapter 14, p 451.
(27) *CRC Handbook*, 51st ed.; CRC Press: Cleveland, OH, 1970; E-71.
(28) Bondi, A. *Physical Properties of Molecular Crystals, Liquids, and Glasses*; John Wiley & Sons, Inc.: New York, 1968; Chapter 14.
(29) The numerical values of the Bondi occupied volumes for the F*n*Cy (n = 3, 4, 6, 8, and 10) repeat units are 155, 180, 231, 282, and 333 Å^3. These calculated volumes are based on substructure volume equivalents of 39.1 Å^3 for the $-CH_2OC{=}N-$ unit and 25.5 Å^3 for the $-CF_2-$ unit determined from Tables 14.1, 14.4, 14.6, 14.9, and 14.14 of reference 28.
(30) A reviewer has suggested that a small quantity of residual organic or inorganic salt from the monomer synthesis and purification might influence the dielectric constant measurement.
(31) Sheehan, D.; Bentz, A. P.; Petropoulos, J. C. *J. Appl. Polym. Sci.* **1962**, *6*, 47.

MA961182D